

RSC Advances

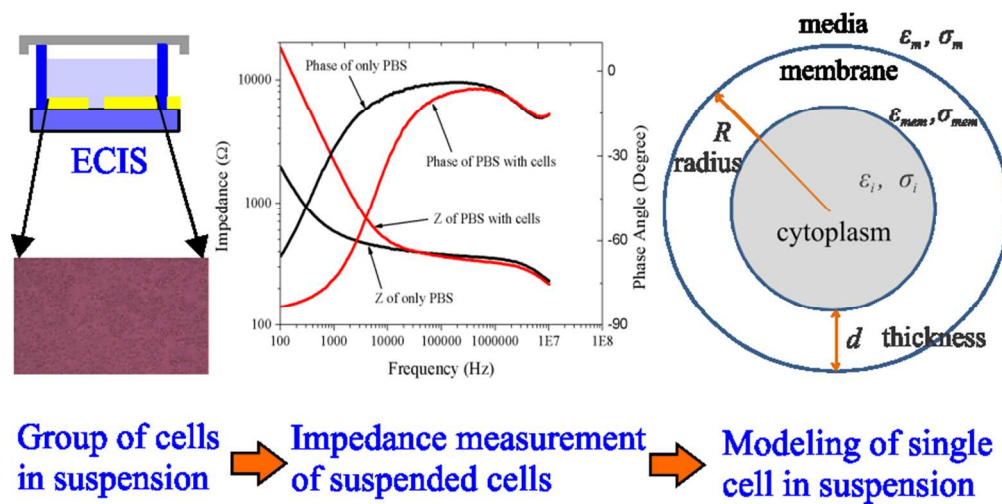


This is an *Accepted Manuscript*, which has been through the Royal Society of Chemistry peer review process and has been accepted for publication.

Accepted Manuscripts are published online shortly after acceptance, before technical editing, formatting and proof reading. Using this free service, authors can make their results available to the community, in citable form, before we publish the edited article. This *Accepted Manuscript* will be replaced by the edited, formatted and paginated article as soon as this is available.

You can find more information about *Accepted Manuscripts* in the [Information for Authors](#).

Please note that technical editing may introduce minor changes to the text and/or graphics, which may alter content. The journal's standard [Terms & Conditions](#) and the [Ethical guidelines](#) still apply. In no event shall the Royal Society of Chemistry be held responsible for any errors or omissions in this *Accepted Manuscript* or any consequences arising from the use of any information it contains.



79x39mm (300 x 300 DPI)

Cite this: DOI: 10.1039/c0xx00000x

www.rsc.org/RSC Advances

PAPER

Evaluation of Single cell electrical parameters from bioimpedance of cells suspension

Debanjan Das*, Farhan Ahmad Kamil, Karabi Biswas, and Soumen Das

Received (in XXX, XXX) Xth XXXXXXXXX 20XX, Accepted Xth XXXXXXXXX 20XX

DOI: 10.1039/b000000x

The present study introduces a simple and detailed analysis technique to extract electrical properties of single cell from impedance spectroscopy data of group of cells in suspension leading to explore a more reliable and cost effective diagnosis process for disease detection. Existing bioimpedance measurement by trapping a single cell in microchannel is quite complex process and suffers from localized joule heating. Considering biological cells show its natural characteristics and functionality in a colony of similar cells rather than individual environment, extraction of single cell electrical parameters from the impedance measurement of group of suspended cells may provide more reliable and effective informations. Experimental and theoretical analysis were performed to extract single cell permittivity, conductivity, membrane capacitance and cytoplasm resistance utilizing established Maxwell's mixture theory. Bioimpedance of suspended HeLa cells were characterized with a controlled volume fraction of cells in the suspension and the measurement was performed by varying the voltage to investigate the change in permittivity and conductivity of HeLa cells. The proposed technique extracted the membrane capacitance and cytoplasm resistance of single HeLa cell to be in 1.8 nF/cm² and 35 kΩ cm² range respectively. Analysis of measured impedance data also reveals that the relative permittivity and conductivity of single HeLa cell is a function of applied potential and frequency.

Introduction

The traditional disease detection techniques require expensive and complex labeling process and extensive biochemical assay. However, the phenomenal progress observed through various experimental results establish that non-biological properties involving mechanical, electrical and optical parameters of cells also modify in disease progression process during pathological changes¹⁻³. Sometimes the signal coming from non-biological parameters may detect early signature of disease before the significant changes observed in biological signal. Therefore, at present a trend has been observed amongst medical research community to explore an alternative label-free, noninvasive detection technique for identifying cancers⁴⁻⁷, bacteria⁸⁻⁹, status of tissues¹⁰⁻¹², cytotoxicity assessment¹³⁻¹⁴, drug screening and toxin detection¹⁵ etc. by quantitative investigation of passive non-biological parameters of cells to enrich clinical processes.

⁴⁰ Electrical Engineering Department,
Indian Institute of Technology Kharagpur 721302, India
Tel.: +919432121661,
Fax: +913222282262
E-mail: debanjands.ee@iitkgp.ac.in

⁴⁵ Electrical Bioimpedance Spectroscopy (EBIS) has been used to characterize complex biological system at the individual cellular level for early diagnosis, prevention and treatment of complex diseases like cancer, malaria, AIDS etc. EBIS is able to produce a signature to distinguish level of disease progress, abnormality of cells and consequently establish a relationship between the electrical properties, biological functions and pathological attributes of cells. Although EBIS technique is continuously exploited for analysis of complex biological systems, its efficacy may further be enhanced through detailed and accurate information of single-cell parameters for reliable diagnosis of diseases. Therefore, analysis of electrical properties of single cell has become a new trend to correlate cellular events for understanding complex physiological processes. In this aspect several experimental and numerical studies for single cell impedance characterization are available in the literature. Jang and Wang¹⁶ performed electrical impedance analysis of single HeLa cell by capturing inside a fabricated three-pillar microstructure in a microchannel. Hua and Pennell¹⁷ fabricated chevron like structure of electrodes in a microfluidic channel to capture single cells and measure the volume changes using impedance. Malleo *et al.* demonstrated a hydrodynamic cell trap system for continuous differential impedance analysis of single

cell¹⁸. The micropipette technique with impedance spectroscopy enables to measure directly the impedance of individual cell membrane, however the technique is invasive since the pipette punctured the cell¹⁹⁻²⁰. Further, new techniques are evolved to measure information of individual single cell in nondestructive way using the microfluidic channel with integrated microelectrodes interfacing the cells directly²¹⁻²³. Planar microhole-based structure has been explored to measure the impedance of single cell without the disturbance of electrode polarization²⁴⁻²⁵. However, the microhole-based method also had a limitation for the interpretation due to the difficulty of observing the exact cellular morphology.

Electrical attributes of single-cell analysis provides information about bio-physiological properties of cell which is sensitive to bio-physical changes in cell. However, this technique suffers from several challenges, which need to be overcome. Handling of single cell in microchannel is complicated and requires trapping mechanisms in the micro-channel for single cell impedance measurement^{16, 26}. The throughput of cell capturing devices is limited unless a large numbers of traps are available in the micro-channel²⁷⁻²⁸. The integration of electrodes together with multiplexed impedance measurements increases the complexity of the system. For large arrays of traps complex active matrix methods is needed to measure the signals from multiple electrodes. Both the large size of cell and its variation in shape together with the difficulty in handling single cell would introduce significant errors into the results. Moreover, microelectrodes enable for only single cell measurement suffers from localized joule heating, produced by highly confined current pathways. Polarization of microelectrodes is also significant and needs special attention to extenuate the effect²⁹⁻³⁰. Furthermore, cells from the same cell line may have different biological status, like in different cell division cycle, in different stage of apoptosis etc. Due to heterogeneity of biological system it is expected that cells show its natural characteristics in a colony of similar cells rather than its individual environment. These shortcomings play major difficulties when the electrical properties are utilized to distinguish between normal and cancerous cells through single cell analysis. Alternatively, electrical properties of single cell can be estimated through the measurement of EBIS of cells in suspensions using well established Maxwell's mixture theory³¹ without interfering the above issues. The analysis relates the complex permittivity of the suspension to the complex permittivity of the particle, the suspending medium and the volume fraction. Therefore, this technique provides a comparatively easy alternative way to extract the single cell parameters without involving the complex technology required for single cell analysis in microchannel.

In the present study, electrical properties of single HeLa cell from the impedance spectroscopy data acquired from its group of cells in suspension have been analyzed. A detailed experimental and theoretical analysis has been performed to extract single cell permittivity, conductivity, membrane capacitance and cytoplasm resistance using Maxwell's mixture theory. EBIS of suspended HeLa cells are measured using an impedance analyzer in the frequency range of 100 Hz to 10 MHz with a controlled volume fraction of cells in the suspension. The experiments were performed for different applied potential to evaluate the

permittivity and conductivity of HeLa cells and then analyzed to extract the single cell parameters. The present study demonstrates a simple and detail analysis technique to extract single cell parameter values from the impedance measurement of group of suspended cells in comparison with other existing techniques involving Maxwell's mixture theory and electrical equivalent circuit models.

Theoretical Modelling

Maxwell's mixture theory

The basic principle of bioimpedance is based on Ohm's law where the potential is measured by applying a small current across a group of cells and subsequently impedance values are determined with a frequency sweep. The recorded bioimpedance is a measure of the complex dielectric properties of the cells which are characterized in terms of permittivity and conductivity. The suspended biological cells in media form a heterogeneous system and its dielectric properties are generally described by Maxwell's mixture theory³¹. For a spherical particle dispersed in a suspending medium at a low volume fraction, the Maxwell's mixture theory provides an equivalent complex dielectric permittivity of the cells in the frequency domain according to eq. 1.

$$\tilde{\epsilon}_{mix} = \tilde{\epsilon}_m \frac{1+2\varphi\tilde{f}_{cm}}{1-\varphi\tilde{f}_{cm}} \quad (1)$$

Where \tilde{f}_{cm} is the complex Clausius–Mossottifactor

$$\tilde{f}_{cm} = \frac{\tilde{\epsilon}_p - \tilde{\epsilon}_m}{\tilde{\epsilon}_p + 2\tilde{\epsilon}_m} \quad (2)$$

The subscripts "mix", "p" and "m" refer to mixture, particle and medium respectively and $\tilde{\epsilon}$ is the complex permittivity and represented as $\tilde{\epsilon} = \epsilon - j\frac{\sigma}{\omega}$, where $j = \sqrt{-1}$, ϵ , σ , ω and φ are permittivity, conductivity and angular frequency, and the volume fraction of the cells in suspension, respectively. Although Maxwell's theory is valid only for low volume fraction ($\varphi < 10\%$), later Hanai and Koizumi³²⁻³³ extended the theory for all volume fractions which is depicted in eq. 3.

$$1 - \varphi = \left(\frac{\tilde{\epsilon}_{mix} - \tilde{\epsilon}_p}{\tilde{\epsilon}_m - \tilde{\epsilon}_p} \right) \left(\frac{\tilde{\epsilon}_m}{\tilde{\epsilon}_{mix}} \right)^{1/3} \quad (3)$$

In terms of single shelled spherical cell model in suspension as shown in Fig.1, the complex permittivity of the cell is³¹:

$$\tilde{\epsilon}_p = \tilde{\epsilon}_{mem} \frac{\gamma^3 + 2 \left(\frac{\tilde{\epsilon}_i - \tilde{\epsilon}_{mem}}{\tilde{\epsilon}_i + 2\tilde{\epsilon}_{mem}} \right)}{\gamma^3 - \left(\frac{\tilde{\epsilon}_i - \tilde{\epsilon}_{mem}}{\tilde{\epsilon}_i + 2\tilde{\epsilon}_{mem}} \right)} \quad (4)$$

with $\gamma = R + d/R$. Where $\tilde{\epsilon}_{mem}$ and $\tilde{\epsilon}_i$ are the complex permittivity of cell membrane and cytoplasm, respectively; R is the radius of cell and d is the membrane thickness. Thus the complex permittivity of the cell, is a function of dielectric properties of membrane, internal properties (mainly cytoplasm), and size of the individual cell. The complex bioimpedance (\tilde{Z}_{mix}) of cells in suspension is related to the equivalent complex permittivity of the mixture and the geometrical parameters of the measurement system by³¹:

$$\tilde{Z}_{mix} = \frac{1}{j\omega\tilde{\epsilon}_{mix}G} \quad (5)$$

where G is a geometric constant, which is the ratio of electrode area (A) to gap (g)- A/g between the electrodes. In this study, impedance spectroscopy of cells suspended in media is carried out using ECIS based device with known geometric constant. Subsequently, complex impedance and equivalent complex permittivity of mixture of suspended cells are found out using eq. 5.

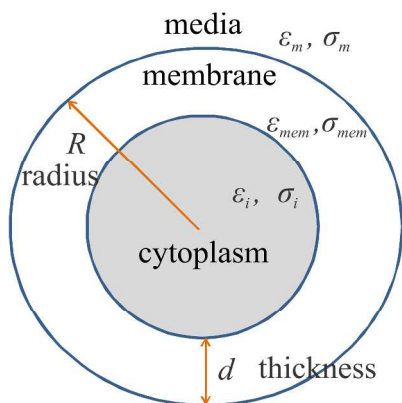


Fig. 1. Schematic diagram of single-shell model of cell in suspension

Equivalent electrical model of single cell

In general an equivalent electrical circuit model analogue to physical model is utilized to describe the electrical properties of suspended cells. Although, it is quite complex to analyze the equivalent circuit model, the conductivity of membrane and the permittivity of the cytoplasm were considered to be very low in the present study to get simple mathematical expression as stated in eq. 6 and 7.

$$\tilde{\varepsilon}_i = -j\sigma_i/\omega. \quad (6)$$

$$\tilde{\varepsilon}_{mem} = \varepsilon. \quad (7)$$

Where σ_i is the conductivity of cytoplasm and ε is the permittivity of membrane. Putting the above assumptions in eq. 4 it can be simplified in eq. 8 and 9.

$$\tilde{\varepsilon}_p = \varepsilon \frac{\gamma^3 + 2 \left(\frac{-j\sigma_i/\omega - \varepsilon}{2\varepsilon - j\sigma_i/\omega} \right)}{\gamma^3 - \left(\frac{-j\sigma_i/\omega - \varepsilon}{2\varepsilon - j\sigma_i/\omega} \right)}. \quad (8)$$

$$\left(\frac{\text{Re}[\tilde{\varepsilon}_p] + j \text{Im}[\tilde{\varepsilon}_p]}{\varepsilon} \right) = \quad (9)$$

$$\left(\frac{2b\varepsilon^2 + a(\sigma_i/\omega)^2}{b^2\varepsilon^2 + (\sigma_i/\omega)^2} \right) + j \left(\frac{\varepsilon\sigma_i/\omega(2-ab)}{b^2\varepsilon^2 + (\sigma_i/\omega)^2} \right),$$

$$\text{where } a = \left(\frac{\gamma^3 + 2}{\gamma^3 - 1} \right), \quad b = \left(\frac{2\gamma^3 + 1}{\gamma^3 - 1} \right) \text{ with } \gamma = \frac{R+d}{R}$$

On dividing the real and imaginary part of $\tilde{\varepsilon}_p$ in eq. 9, a quadratic equation is obtained as:

$$\frac{a}{\omega} (\sigma_i/\varepsilon)^2 - K(2-ab)(\sigma_i/\varepsilon) + 2b\omega = 0, \quad (10)$$

$$\text{where } K = \left(\frac{\text{Re}[\tilde{\varepsilon}_p]}{\text{Im}[\tilde{\varepsilon}_p]} \right)$$

On assuming the $l = \sigma_i/\varepsilon$ and equating the imaginary part of eq. 9 the permittivity of single cell is obtained

$$\varepsilon = \left(\frac{b^2 + (l/\omega)^2}{(l/\omega)(2-ab)} \right) \text{Im}[\tilde{\varepsilon}_p]. \quad (11)$$

Using eq. 10 value of l is calculated, then the relative permittivity (ε) is obtained from eq. 11, and finally conductivity (σ_i) is incurred through $\sigma_i = l \times \varepsilon$.

The impedance of cell suspension consists of impedance of the medium represented by a parallel combination of resistance and capacitance, and impedance of cells. According to Foster and Schwan³⁴ a single cell is approximated to a cytoplasm resistor (R_i) in series with a membrane capacitor (C_{mem}) as represented in Fig. 2. The cell membrane consists of a thin phospholipid bilayer having very low conductivity and acts as a dielectric material offering a capacitive pathway to the system.

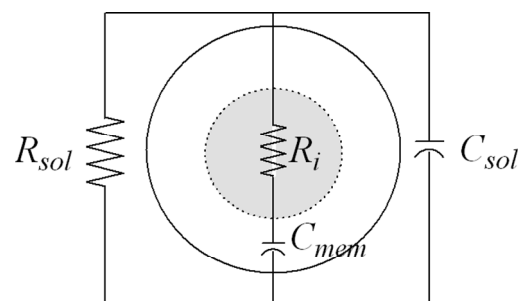


Fig. 2. Simplified equivalent circuit model of a single cell in suspension

The cell cytoplasm can be approximated as a highly conducting ionic solution with a large concentration of dissolved organic material which is considered to be resistive path way to the electrical signal in the electrical equivalent of the system. The values of simplified frequency dependent cell parameters are determined by the dielectric and conductivity properties of cell and medium, cell size, volume fraction and geometric constant of the EBIS system³¹:

$$C_{mem}(\omega) = \frac{9\varphi R \varepsilon}{4d} G. \quad (12)$$

$$R_i(\omega) = \frac{4 \left(\frac{1}{2\sigma_m} + \frac{1}{\sigma_i} \right)}{9\varphi G}. \quad (13)$$

The frequency dependent relative permittivity (ε) and conductivity (σ_i) of single cell obtained in eq. 10 and 11 are used in eq. 12 and 13 to extract the single cell membrane capacitance and cytoplasm resistance.

Materials and Methods

Cell Suspension Preparation

In the present study, bioimpedance spectroscopy was performed on HeLa cell line suspended in PBS buffer solution. HeLa cells are the cell line of human cervical carcinoma, which is one of the leading causes of death among women all over the world. HeLa cells were cultured in MEM media supplemented with 10% heat-inactivated fetal bovine serum, L glutamine, pyruvic acid, and 1% antimycotic antibiotic. The cells were grown in a humidified atmosphere containing 5% carbon dioxide at 37°C. The confluent cell population was removed by treating with 0.25% trypsin and 0.02% EDTA for 5 min. Subsequently, the cells with 10^6 numbers of population were re-suspended in

400 μL of fresh PBS buffer media having pH value 7.4 and conductivity 1.56 S/m and bioimpedance spectroscopy of the suspended cells were performed using ECIS based device.

Electrical Bioimpedance Spectroscopy

The impedance measurement of cell suspensions was carried out in ECIS-8W1E DD (Applied BioPhysics, USA) cell culture well. Agilent precision impedance analyzer 4294-A was used to record the impedance data from the ECIS device. The ECIS-8W1E DD culture well consists of eight separate mini-culture wells having an individual circular shape working electrode (WE) and common counter electrode (CE) made of thin gold film. However a portion of the individual WE is coated with a biocompatible polymer keeping a 250 μm diameter circular exposed part at the centre of WE to minimize electrode-media interface. The ECIS device ECIS-8W1E DD was mounted on a PCB and necessary electrical connections were taken to connect it with the impedance analyzer. Initially, 400 μL of PBS media was added into one of the wells of the ECIS device and impedance-phase angle values were measured. This serves as control and baseline of the impedance measurement system in the absence of HeLa cells. Subsequently, HeLa cells suspended in 400 μL of PBS media was added into the wells of the ECIS device for impedance spectroscopy. The impedance magnitude and phase angle were recorded using Agilent precision impedance analyzer 4294-A in the frequency range of 100 Hz to 10 MHz for different excitation voltage from 10 mV to 1 V peak-peak. The each measurement was also repeated for three times without disturbing the ECIS system. There are 167 data points measured in entire frequency range. The average recorded data were then analyzed using Maxwell's Mixture Theory and equivalent circuit model to extract the electrical parameters of single HeLa cell.

Algorithm to calculate single cell electrical parameters

In the present parameter extraction technique, the complex bioimpedance of group of suspended cells having a known volume fraction is measured then the following steps has performed to extract electrical properties of single cell:

- Calculated the complex permittivity of the cell mixture ($\tilde{\epsilon}_{\text{mix}}$) using eq. 5. with a given geometric constant (G).
- Estimated the complex permittivity of the single cell ($\tilde{\epsilon}_p$) using already calculated $\tilde{\epsilon}_{\text{mix}}$ and known value of $\tilde{\epsilon}_m$ and volume fraction (ϕ) according to eq. 3.
- The relative permittivity of membrane (ϵ) and conductivity of cytoplasm (σ_c) of single cell is determined by using eq. 10 and 11.
- Extracted the membrane capacitance and cytoplasm resistance of single cell using eq. 12 and 13.

Results and Discussion

Impedance of HeLa cells in suspension

Fig. 3 shows the Bode diagram of impedance magnitude and phase angle variation with frequency for both PBS media without and with suspended HeLa cells at the operating voltage of 10 mV. The Bode magnitude of only PBS media without cells decreases with increasing frequency, representing a transition from capacitive to resistive behavior as the applied signal moves from

low to high³⁵. Phase plot shows that phase angle of only PBS media without cells moves towards zero degree with increasing frequency. Fig. 3 also shows the effects of adding HeLa cells to the PBS media on impedance data. Since, media is more conducting than the suspended HeLa cells, impedance of media is lower and phase angle of media is less negative than that of cells with suspended media. The Bode diagram depicts that on adding the cells to the media the impedance value increases abruptly at lower frequencies (<100 kHz), while both the curves coincide at higher frequencies. Similarly, phase angle decreases at lower frequency for media with cells, while two phase curves coincide at higher frequency. This experimental observation indicates that HeLa cells influence the impedance data at lower frequency. In EBIS system coating capacitance is formed due to thin polymer layer on the electrode surface and is in nF range resulting its dominance in higher frequency zone. Besides that solution resistance also plays a dominant role in higher frequency. Therefore, coating capacitance and solution resistance behave as RC circuit in higher frequency leading to the coincidence of all the curves without changing the impedance spectrum.

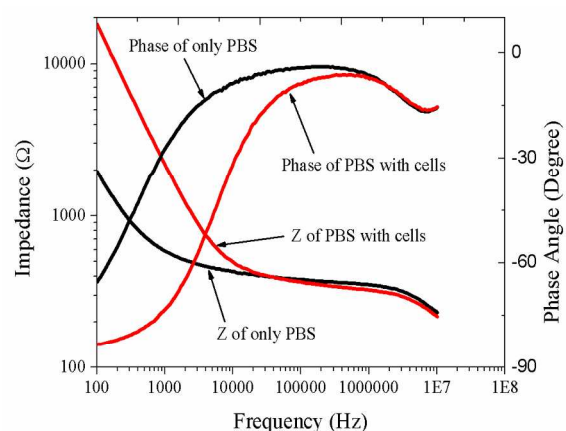


Fig. 3. Bode diagram of ECIS system with and without cells suspended in PBS solution

Fig. 4 shows the variation of magnitude and phase of impedance, at different voltage level varying from 10 mV to 1 V. At all the operating potential the impedance magnitude of suspended HeLa cells decreases and phase angle increases with increasing frequency. The impedance values decreases rapidly in the lower frequency range (<100 kHz), while all the curves coincide at higher frequency range. The Fig. 4a also indicates that the impedance magnitude decreases with increasing applied potential e.g. at 1 kHz the impedance of suspended HeLa cells reduces from 2.2 k Ω to 702 Ω with increased potential from 10 mV to 1 V. Similarly, phase angle value decreases with higher applied voltage as observed in Fig. 4b. This observation is attributed due to opening of more ionic channels of the cell membrane at higher voltages, influencing the permittivity of cell membrane and conductivity of cell cytoplasm^{16,36}. It is expected that higher electric field will greatly influence the ion exchange process between the intra- and extra-cellular solution which leads to achieve lower impedance and higher (more positive) the phase angle of cells³⁷. However at 1V the initial impedance value was quite low as compared to lower operating voltage but follows the similar trend of variation with increase of frequency as observed in Fig. 4a. The lower impedance value is attributed for breakdown of membrane dielectric due to high electric field which is maintained throughout the entire frequency range. The coincidence of all the impedance curves above 10 kHz and thereby maintaining a near equal impedance value at higher

frequency range represents the coating capacitance of ECIS system which does not alters with applied voltage.

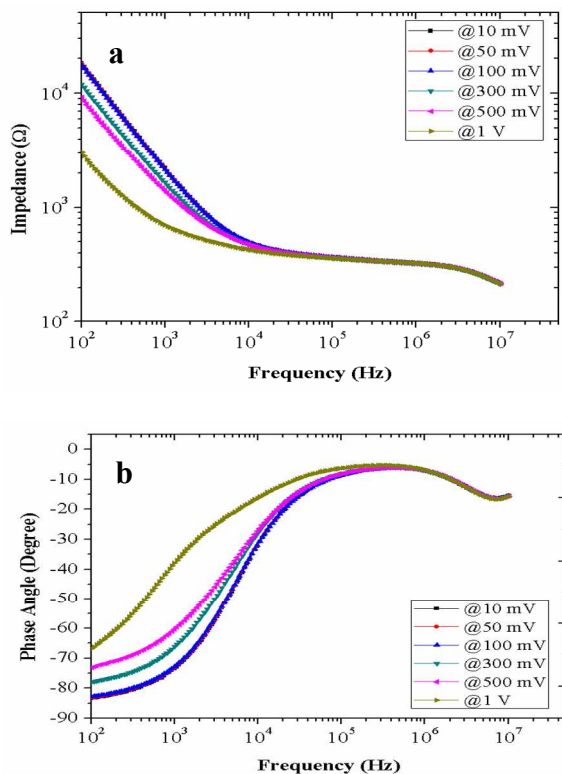


Fig. 4. (a) Impedance magnitude spectroscopy of suspended HeLa cells at different operating potential, (b) Variation of phase of HeLa cells in suspension at various voltages

Extraction of single cell parameters

Maxwell's mixture theory has been explored for single cell analysis utilizing the impedance data measured at various voltages. In this approach, volume fraction of 1 million HeLa cells suspended in a total volume of 400 μL is represented as:

$$\phi = \frac{10^6 \times \left(\frac{4}{3}\right) \pi R^3}{400 \times 10^{-6} \times 10^{-3}} \approx 0.0104 < 0.1. \quad (14)$$

Considering the radius of a HeLa cell (R) is 10 μm while the typical thickness of membrane (d) is 5 nm³⁷. The geometric constant ($G=A/g$) of ECIS as mentioned in eq. 5 is not easy to find because of non-linear electric field. However the approximate value of G is found out by substituting the area of the electrode (A) equal to 1 cm^2 and average gap between the electrodes (g) to 3 mm. The measured relative permittivity of PBS medium used in the experiment is 136, and the conductivity of medium is 1.56 S/m. Hence the complex permittivity of PBS may be expressed as eq. 15.

$$\tilde{\epsilon}_m = 136\epsilon_0 + j \frac{1.56}{\omega} \quad (15)$$

where $\epsilon_0 = 8.854 \times 10^{-12}$ F/m and ω is angular frequency. Using impedance spectroscopy data obtained from the experiment, the complex permittivity of mixture ($\tilde{\epsilon}_{\text{mix}}$) was calculated using eq.

5 as given in section 2. Subsequently, $\tilde{\epsilon}_{\text{mix}}$, $\tilde{\epsilon}_m$ and ϕ were substituted in eq. 3 to estimate the complex permittivity ($\tilde{\epsilon}_p$) of single HeLa cell. The Fig. 5a and 5b illustrates the variation of

conductivity and permittivity of the single HeLa cell, respectively with the frequency sweep from 100 Hz to 10 MHz for various operational voltages in the range of 1 mV-1 V. The results show that both the conductivity and relative permittivity of equivalent single HeLa cell increase with higher operational voltage at lower frequency range.

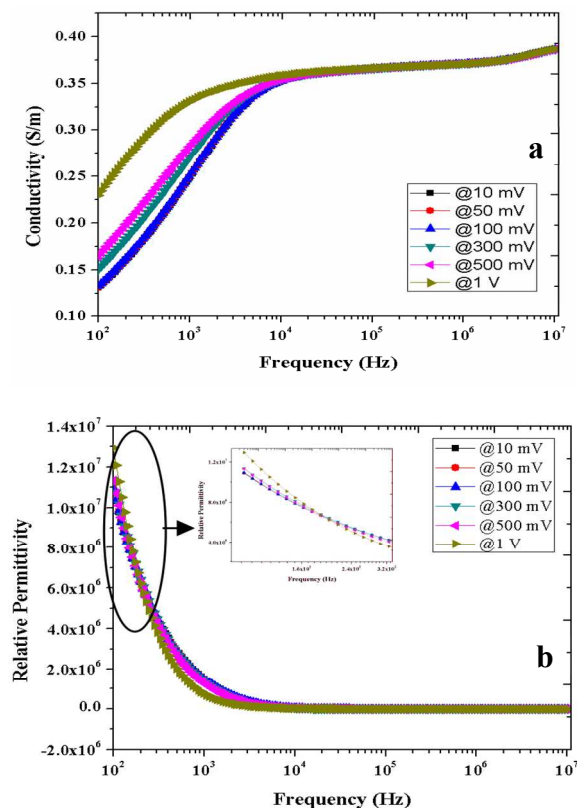


Fig. 5. Variation of (a) Conductivity, (b) Relative permittivity of single HeLa cell with frequency at different voltages

From Fig. 5a it may be observed that, at lower frequency, the conductivity of single HeLa cell increases from 0.13 S/m to 0.23 S/m as the voltage increased from 10 mV to 1V. The results indicate that the higher electric field opens up more ionic channels in the cell membrane and thus enhances the charge exchange process between cytoplasm and extracellular solution. This phenomenon allows higher current to flow through cell membrane and cytoplasm leading to increase of conductivity. Availability of ionic channel enhances the charge exchange between the cytoplasm and extra-cellular solution. Wang and Jang³⁷ showed similar variation of permittivity and conductivity for different voltages measured by trapping a single HeLa cell inside the microchannel. Fig. 5b shows that the measured relative permittivity of single HeLa cell is nearly same for different operating voltage upto 300 mV. At higher applied voltage above 300 mV, the slope of relative permittivity of cell is sharper than lower voltage data upto 4 kHz and thereafter all the permittivity data remain nearly same for entire operating voltages. Under higher electric field the capacitance representing the cell membrane may be fully charged at lower operating frequency, whereas at higher frequency zone it is unable to be fully charged within one cycle³⁷⁻³⁸. This demonstrates the decrease in relative permittivity of HeLa cell with increasing frequency at higher operating potential. The above experimental facts depicts that the relative permittivity and conductivity of single HeLa cell are a function of applied potential and frequency. These informations

may be useful for electroporation of cell membrane and characterization of different diseased cells.

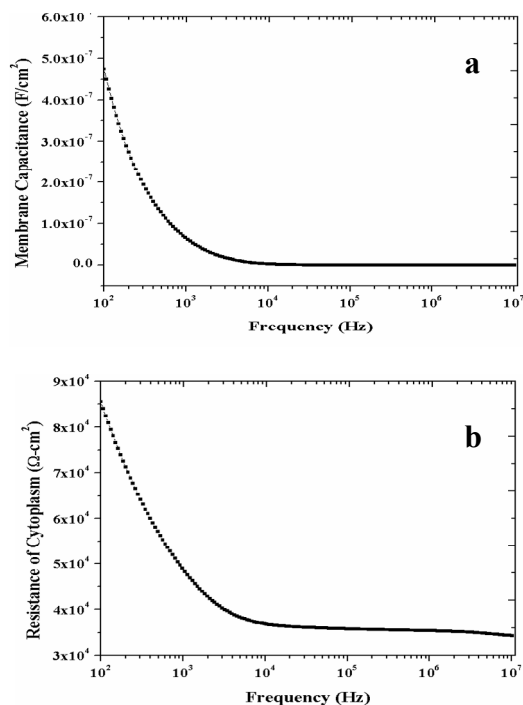


Fig. 6. Variation of (a) Membrane capacitance, (b) cytoplasm resistance with respect to frequency

Additionally the parameters such as cell membrane capacitance and cytoplasm resistance of a cell may be utilized for identification of cell type and may also be explored for diagnostic and prognostic applications correlating with the disease progression. Therefore, extraction of membrane capacitance and cytoplasm resistance of single cell has emerged as major requirement to get the detailed insight of the disease and characterize them. The already extracted relative permittivity (ϵ) and conductivity (σ) of single cell are further used to obtain the membrane capacitance and cytoplasm resistance of single HeLa cell using eq. 12 and 13 and its variation with frequency are shown in Fig. 6a and 6b, respectively.

Since the permittivity of membrane decreases continuously with the frequency, the membrane capacitance shows similar variation as observed in Fig. 6a. Its value decreases from 50 nF/cm² at 100 Hz to 9 pF/cm² at 1 MHz. In β -dispersion range (above 100 kHz) the membrane capacitance becomes almost constant in the range of few nF/cm², which matches closely with the generally accepted value of single HeLa cell membrane capacitance obtained by cell trapping¹⁶. As depicted from the Fig. 6b cytoplasm resistance decreases with frequency in lower frequency range while it becomes almost constant (35 k Ω .cm²) in β -dispersion range which is also congruent with the generally accepted values of single HeLa cell cytoplasm resistance obtained by the method of cell trapping¹⁶. Table 1 shows a comparison between the extracted cell membrane capacitance and cytoplasm resistance through single cell trapping method by Wang and Jang³⁷ and our method of impedance measurement of colony of suspended cells. Therefore, the experimental and theoretical analysis presented in this paper exhibits that electrical properties of single cell may be evaluated through the measurement of EBIS of a colony of cells in suspensions using well established Maxwell's mixture theory and avoids complicated single cell trapping for impedance study. It is expected that the extracted

parameters will provide more realistic and practical information about the cell because its measurement has conducted in close resemblance to ambient conditions. Although the present study demonstrated the feasibility of this technique for one type of cells, the validity and repeatability of this approach requires further confirmation using a variety of cells.

Table I. Comparison of extracted single cell parameters

Single cell parameters	By single cell trapping method(Wang)	By cells suspension method
Resistance of cytoplasm (Ω . cm ²)	6.0×10^4	3.5×10^4
Membrane capacitance (F/cm ²)	2.5×10^{-9}	1.8×10^{-9}

Conclusion

In this study, electrical properties of single HeLa cell were extracted through bioimpedance analysis of its colony of cells in suspension by Maxwell's mixture theory. Using the bioimpedance spectroscopy data of HeLa cells in PBS medium at 50 different voltages, complex permittivity of the mixture was calculated which was further analyzed to extract the permittivity and conductivity of single HeLa cell. The experimental observation reveals that the relative permittivity and conductivity of single HeLa cell is a function of applied potential and frequency. At low frequency, the conductivity of single cell increases from 0.13 S/m to 0.23 S/m as the voltage increased from 10 mV to 1V which is attributed for opening of more ion channels of membrane at higher electric field, allowing higher current to flow through the cell membrane and cytoplasm leading to increase of conductivity. At lower frequencies the relative permittivity of cell membrane decreases with the voltage. Relative permittivity of single HeLa cell is almost constant at the entire frequency range at lower operating voltage of 10 mV-300 mV, while at higher applied voltage at 500 mV and 1 V, it reduces rapidly with increasing frequency. This indicates that under higher electric field the capacitance representing the cell membrane may be fully charged at lower operating frequency, whereas at higher frequency zone it may be unable to be fully charged within one cycle. In β -dispersion range the membrane capacitance and cytoplasm resistance were calculated to be in 1.8 nF/cm² range and 35 k Ω .cm² range respectively, which matches closely with the value obtained from cell trapping method found in literature. Therefore, the present study provides an alternative technique to extract electrical properties of single cell from the bioimpedance spectroscopy of a colony of cells in suspension by avoiding the complexity of single cell capturing and impedance measurement in microchannel.

Acknowledgement

The authors would like to acknowledge the staff members of MEMS & Microelectronics Laboratory of ATDC for their help. The authors would also like to thank the staff members of Cell Culture Group of SMST for providing the cell line to conduct the experiment.

References

1. Y. Bishitz, H. Gabai, P. Girshovitz and N. T. Shaked, *Journal of Biophotonics*, 2013.
2. A. Rehman, S. Firdous, M. Nawaz and M. Ahmad, *Laser Phys.*, 2012, **22**, 322-326.
3. L. Yang, L. R. Arias, T. Lane, M. Yancey and J. Mamouni, *Anal Bioanal Chem*, 2011, **399**, 1823-1833.
4. A. J. Surowiec, S. S. Stuchly, J. R. Barr and A. Swarup, *Biomedical Engineering, IEEE Transactions on*, 1988, **35**, 257-263.
5. J. Jossinet and M. Schmitt, *Annals of the New York Academy of Sciences*, 1999, **873**, 30-41.
6. R. J. Halter, A. Schned, J. Heaney, A. Hartov, S. Schutz and K. D. Paulsen, *The Journal of Urology*, 2008, **179**, 1580-1586.
7. H. Dieter, S. T. Staelin, J. Z. Tsai, S. Tungjitkusolmun, D. M. Mahvi and J. G. Webster, *Physiological Measurement*, 2003, **24**, 251.
8. M. Varshney and Y. Li, *Biosensors and Bioelectronics*, 2009, **24**, 2951-2960.
9. S. M. Radke and E. C. Alocilja, *Biosensors and Bioelectronics*, 2005, **20**, 1662-1667.
10. S. S. Swarup A, Surowiec A., *Bioelectromagnetics*, 1991, **12**, 1-8.
11. C. Gabriel, S. Gabriel and E. Corthout, *Physics in Medicine and Biology*, 1996, **41**, 2231.
12. M. R. Stoneman, M. Kosempa, W. D. Gregory, C. W. Gregory, J. J. Marx, W. Mikkelson, J. Tjoe and V. Raicu, *Physics in Medicine and Biology*, 2007, **52**, 6589.
13. J. Müller, C. Thirion and M. W. Pfaffl, *Biosensors and Bioelectronics*, 2011, **26**, 2000-2005.
14. C. Xiao and J. H. T. Luong, *Toxicology and Applied Pharmacology*, 2005, **206**, 102-112.
15. F. Asphahani and M. Zhang, *Analyst*, 2007, **132**, 835-841.
16. L.-S. Jang and M.-H. Wang, *Biomed Microdevices*, 2007, **9**, 737-743.
17. S. Z. Hua and T. Pennell, *Lab on a Chip*, 2009, **9**, 251-256.
18. D. Malleo, J. T. Nevill, L. Lee and H. Morgan, *Microfluid Nanofluid*, 2010, **9**, 191-198.
19. S. Takashima, K. Asami and Y. Takahashi, *Biophysical Journal*, 1988, **54**, 995-1000.
20. K. Asami, Y. Takahashi and S. Takashima, *Biophysical Journal*, 1990, **58**, 143-148.
21. H. E. Ayliffe, A. Bruno Frazier and R. D. Rabbitt, *Microelectromechanical Systems, Journal of*, 1999, **8**, 50-57.
22. A. Han and A. B. Frazier, *Lab on a Chip*, 2006, **6**, 1412-1414.
23. Y. H. Cho, T. Yamamoto, Y. Sakai, T. Fujii and K. Beomjoon, *Microelectromechanical Systems, Journal of*, 2006, **15**, 287-295.
24. R. Díaz-Rivera and B. Rubinsky, *Biomed Microdevices*, 2006, **8**, 25-34.
25. S. Cho and H. Thielecke, *Biosensors and Bioelectronics*, 2007, **22**, 1764-1768.
26. A. Han, L. Yang and A. B. Frazier, *Clinical Cancer Research*, 2007, **13**, 139-143.
27. D. D. Carlo, L. Y. Wu and L. P. Lee, *Lab on a Chip*, 2006, **6**, 1445-1449.
28. O. K. A. Skelley, H. Suh, R. Jaenisch, J. Voldman, *Nat Methods*, 2009, **6**, 147-152.
29. H. P. Schwan, *Ann Biomed Eng*, 1992, **20**, 269-288.
30. A. R. Abdur Rahman, D. T. Price and S. Bhansali, *Sensors and Actuators B: Chemical*, 2007, **127**, 89-96.
31. T. Sun and H. Morgan, *Microfluid Nanofluid*, 2010, **8**, 423-443.
32. T. Hanai, N. Koizumi and A. Irimajiri, *Biophys. Struct. Mechanism*, 1975, **1**, 285-294.
33. T. Hanai, K. Asami and N. Koizumi, *Bull. Inst. Chem. Res.*, 1979, **57**, 297-305.
34. K. R. Foster and H. P. Schwan, *Critical Reviews™ in Biomedical Engineering*, 1989, **17**, 25-104.
35. A. R. A. Rahman, L. Chun-Min and S. Bhansali, *IEEE Transactions on Biomedical Engineering*, 2009, **56**, 485-492.
36. J. C. Weaver and Y. A. Chizmadzhev, *Bioelectrochemistry and Bioenergetics*, 1996, **41**, 135-160.
37. M.-H. Wang and L.-S. Jang, *Biosensors and Bioelectronics*, 2009, **24**, 2830-2835.
38. S. G. Orjan G. Martinsen, *Bioimpedance and Bioelectricity Basics*, Second Edition edn., Academic Press, London, UK, 2008.